Processing and Application of Ceramics 14 [2] (2020) 128–133
https://doi.org/10.2298/PAC2002128H

Preparation and characterization of porous Al_2O_3 based on nano-Al_2O_3 powders and PLA template by microwave sintering

Zhenhua He*, Shifei Zhu, Canhui Liu

School of Information Engineering, Wuhan University of Technology, Wuhan 430070, PR China

Received 4 April 2019; Received in revised form 26 September 2019; Received in revised form 23 February 2020; Accepted 31 March 2020

Abstract

Macroporous and mesoporous Al_2O_3 body was prepared using mesh screening shaped polylactic acid (PLA) template. The mesh screening shaped PLA template was made from 3D cylindrical model by adjusting the PLA filling rate at 30 vol.%. After 3D printing, the PLA template was filled with Al_2O_3 nano-powders and microwave sintered at 1673 K for 20 min. During the sintering, the PLA template was decomposed and left large pores which could promote sintering of Al_2O_3. The Al_2O_3 sintered body showed macroporous structure with the pore size of 100 to 300 nm and also mesoporosity with local single crystal structure. The average pore diameter of mesoporous structures in the Al_2O_3 sintered body was about 7.6 nm. The Vickers hardness of the porous Al_2O_3 is 1.254 ± 0.039 GPa. The obtained results confirmed that 3D-printed PLA template assisted microwave sintering is a promising technical processing for the fabrication of macroporous and mesoporous Al_2O_3 with local single crystal structure.

Keywords: *porous Al_2O_3, 3D printing, microwave sintering, advanced manufacturing*

I. Introduction

Porous materials have lots of specific properties, such as high surface area, high permeability, low density, low specific heat and low thermal conductivity [1]. Because of these characteristics, porous materials have attracted considerable attentions as a new class of materials for a wide range of applications, for instance, bone substitutes, automotive industry, catalyst supports, filters for molten metals and hot gases, refractory linings for furnaces, porous implants in the area of biomaterials etc. [2–5].

Alumina (Al_2O_3) has high melting point, high hardness, high strength, high chemical stability, low density, superior wear and corrosion resistance, bio-inertness, high thermal conductivity and high oxidation resistance [6–8]. Specifically, porous Al_2O_3 has attracted the attention and interest of scientists all over the world. Sepulveda *et al.* [1] fabricated porous Al_2O_3 materials using foaming and in situ polymerisation of organic monomers technique. The porous Al_2O_3 showed cellular structure and the cell size of sintered bodies was enlarged from 30–600 μm in non-expanded foams up to 50–2000 μm in expanded foams. Deville *et al.* [3] prepared porous Al_2O_3 materials by ice-templated freeze casting. The porous Al_2O_3 showed multilayered structure, the structure wavelength was ranged from 2 to 130 μm. Luyten *et al.* [9] prepared porous Al_2O_3 materials by reaction bonding modified polyurethane technique and gel casting. The porous Al_2O_3 bodies showed cellular structure. The cell size in Al_2O_3 sintered bodies by reaction bonding modified polyurethane technique was ranged from 400 to 1300 μm. On the other hand, the cell size in Al_2O_3 sintered bodies by gel casting was ranged from 50 to 800 μm. Tang *et al.* [10] prepared porous Al_2O_3 materials by freeze casting using TBA-sucrose-water system as solvents in the slurries and annealing at low temperature. The pores in sintered bodies showed small cylindrical structure, the median pore size was ranged from 2.6 to 6.9 μm. Li *et al.* [11] prepared anodic porous alumina (AAO) by electrochemical oxidation method. The pores in AAO showed two-dimensional hexagonal arrangement and the interpore distance ranged from 50 to 420 nm.

* Corresponding authors: tel: +86 18571525933,
e-mail: *zhenhuahe@whut.edu.cn*

In this study, we propose a new method, which combines additive manufacturing (3D printing) technique and microwave sintering technique, to prepare porous Al_2O_3. 3D-printed polylactic acid (PLA) template was designed to obtain a three dimensional stacking structure. The structure of PLA template filled with nano-Al_2O_3 powder was properly designed to obtain open cell structure in Al_2O_3 sintered bodies. The PLA template was not only designed to keep supporting structure before sintering, but also to be used to keep enough space to help the rearrangement of Al_2O_3 particles during the microwave sintering for the synthesis of single crystal Al_2O_3. During sintering in the air atmosphere, the PLA template was completely decomposed into H_2O and CO_2 at high temperature (above 1273 K).

3D printing is a new rapid fabricating technique without material removal processes. It is very suitable for producing parts with complex geometry that are difficult to obtain using material removal processes [12]. Microwave sintering technique has the advantages of energy saving, fast heating rate, short soaking time and low sintering temperature, which can prevent grain growth during the sintering process [13]. The microwave sintering was used to inhibit the grain growth of Al_2O_3 during sintering. The crystal structure, microstructure and surface atomic arrangement of Al_2O_3 sintered body by microwave sintering using 3D-printed PLA template were investigated.

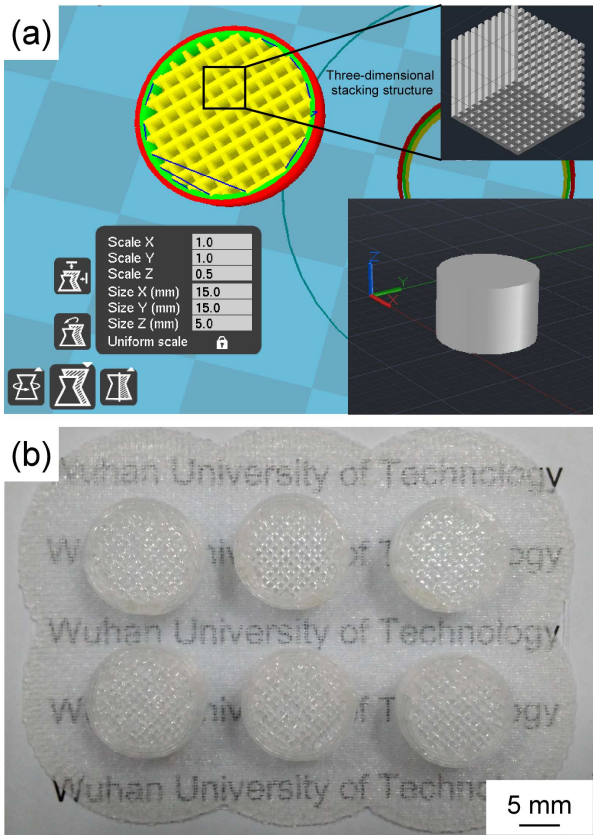

Figure 1. Simulation graphics in Cura software for 3D printing of the PLA cylindrical template (a) and produced 3D-PLA stacking structures (b)

II. Experimental procedure

In the first step, a cylindrical polylactic acid (PLA) template with three dimensional stacking structure (Fig. 1) was fabricated by 3D printing. Circular cylinder model was drawn by CAD software. The 3D model file from CAD software was imported into Cura software, where the diameter and height of the circular cylinder were set to 15 mm and 5 mm, respectively. The 3D printing filling rate was set to 30 vol.% while the filling rate of bottom layer was set to 100 vol.%. The polylactic acid 3D template was prepared by Fused Deposition Model (FDM) 3D Printer (STUDE II, Wuhan Stude 3D Technology Co. Ltd., China). The raw material for FDM 3D Printer was PLA (polylactic acid, 99% purity, 1.75 mm in diameter of coiling wire, Shenzhen Creality 3D Technology Co. Ltd., China).

After 3D printing, the PLA template was filled with Al_2O_3 powder (99.9% purity, 30 nm average grain size, α-phase was main crystal structure, Aladdin Reagent Shanghai Co. Ltd., China). The PLA template filled with nano-Al_2O_3 powder was pressed in steel die of 20 mm diameter for 180 s at 30 MPa. The obtained sample was consolidated at 1673 K under air atmosphere in the microwave muffle furnace (HAMiLab-M1500, Synotherm Corporation, China). The heating rate was 0.20 K/s (298 K to 1373 K) and 0.08 K/s (1373 K to 1673 K). The soaking time of microwave sintering was 20 min.

The thermogravimetric (TG) and differential scanning calorimeter (DSC) analysis were performed by Synchronous Thermal Analyzer (STA 449F3, NETZSCH, Germany). The crystal structure was investigated by X-ray diffraction (XRD, Empyrean, PANalytical B.V., Netherlands) with Cu Kα radiation. Field emission scanning electron microscopy (FE-SEM, JSM-7500F, JEOL, Japan) and transmission electron microscopy (TEM, JEM-2100F, JEOL, Japan) were used to examine the microstructure of the porous nano-Al_2O_3 sintered body. TEM samples were prepared by grinding the Al_2O_3 sintered body into powder and uniformly dispersing it in ethyl alcohol by ultrasound for 10 min. Drop of this suspension was put on the copper mesh with amorphous carbon film which was used for analyses after drying. The specific surface area and mesoporous pores distribution of Al_2O_3 sintered body by low-temperature nitrogen adsorption or desorption was tested by ASAP 2460 (Micrometrics, USA) analyser. Vickers hardness (H_v) was determined at room temperature at 5 points on the sample using a digital Vickers microhardness tester (VH1202, Wilson, USA) at loads (P) of 2.94 N.

III. Results and discussion

The circular cylinder model was drawn as shown in Fig. 1a in Cura software for 3D printing. The diameter, height and filling rate of the model were set to 15 mm, 5 mm and 30 vol.%, separately. The filling rate of bot-

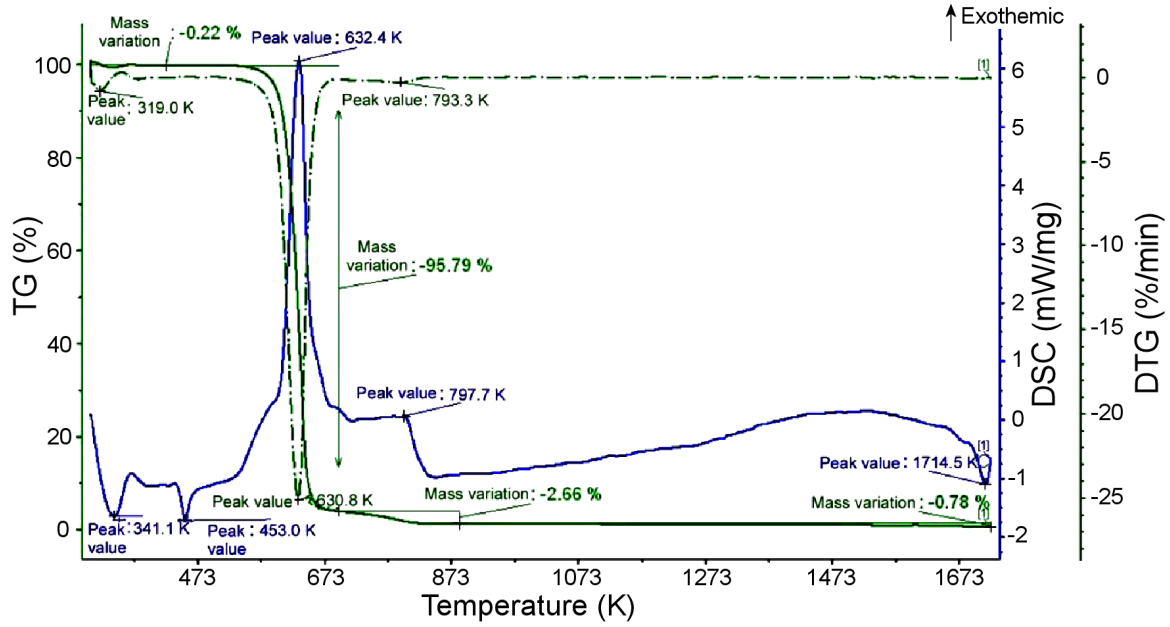

Figure 2. TG and DSC results of 3D-printed polylactic acid template (in temperature range from 298 to 1723 K, heating rate was 0.17 K/s in air environment)

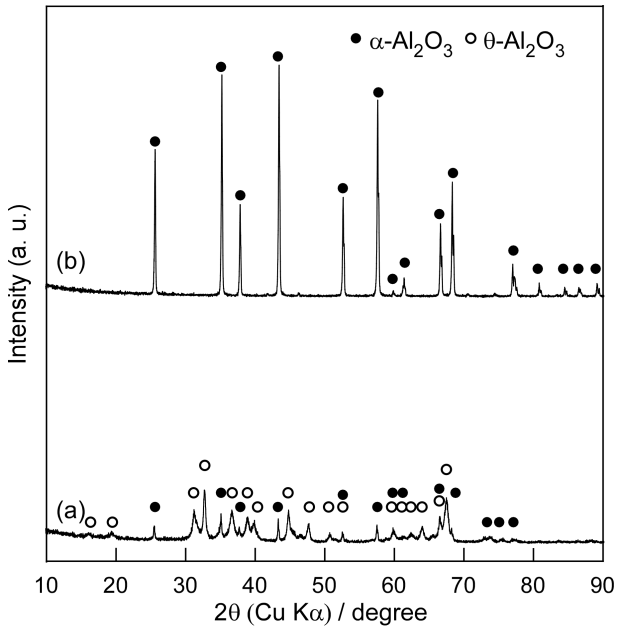

Figure 3. XRD patterns of raw nano-Al_2O_3 powder (a) and Al_2O_3 body microwave sintered at 1673 K (b)

tom and side of the model were set to 100 vol.%. Figure 1b shows the six 3D printed polylactic acid (PLA) templates with three dimensional stacking structures. The diameter of stacking unit is about 0.4 mm according to the nozzle size of the 3D printing machine. The total manufacturing time of the printed PLA template as shown in Fig. 1b was 15 min.

Figure 2 shows the thermogravimetric (TG) and differential scanning calorimeter (DSC) testing results of the single 3D-printed PLA template in temperature range from 298 to 1723 K under air environment. The temperature range of rapid mass variation of the PLA template was from 473 to 873 K. The peak value of the mass variation was at 630.8 K. The total mass loss of the PLA template was 99.45 wt.%. The mass loss of the PLA template, in temperature range from 298 to 1673 K, was above 99 wt.%. The oxidation products of the pure PLA at high temperature are CO_2 and H_2O. Since PLA can be extracted from plants, 3D-printed PLA template has the characteristics of environmental friendliness [14].

Figure 3 shows the XRD results of the raw nano-Al_2O_3 powder and Al_2O_3 sintered body. The XRD pattern of the raw nano-Al_2O_3 powder is assigned to α- and θ-Al_2O_3, whereas the XRD pattern of Al_2O_3 sintered body is attributed to pure α-Al_2O_3. The increasing of relative intensity of α-Al_2O_3 and disappearing of θ-Al_2O_3 (Fig. 3) indicated a phase transformation of θ-Al_2O_3 into α-Al_2O_3 in microwave sintering at 1673 K. No impurity phases, such as carbon, were identified.

Figure 4 shows the FE-SEM microstructures of the raw nano-Al_2O_3 powder and Al_2O_3 sintered body. Figures 4a and 4b show the agglomeration state of the raw Al_2O_3 powder and confirm that the average particle size of the raw nano-Al_2O_3 powder was about 30 nm. The agglomeration state may be caused by the nano-size diameter and huge specific surface area of the raw Al_2O_3 powder. As shown in Figures 4c and 4d, the porous structure of the Al_2O_3 sintered body after microwave sintering at 1673 K was obtained. The average grain size of the porous Al_2O_3 sintered body was 100–150 nm and the pore diameters were 100–300 nm. According to the pore size it can be confirmed that the Al_2O_3 sintered body has macroporous structure. The grain growth from 30 nm to 100–150 nm of Al_2O_3 sintered body after microwave sintering was observed. After the sintering at 1673 K in air, the PLA template was completely decom-

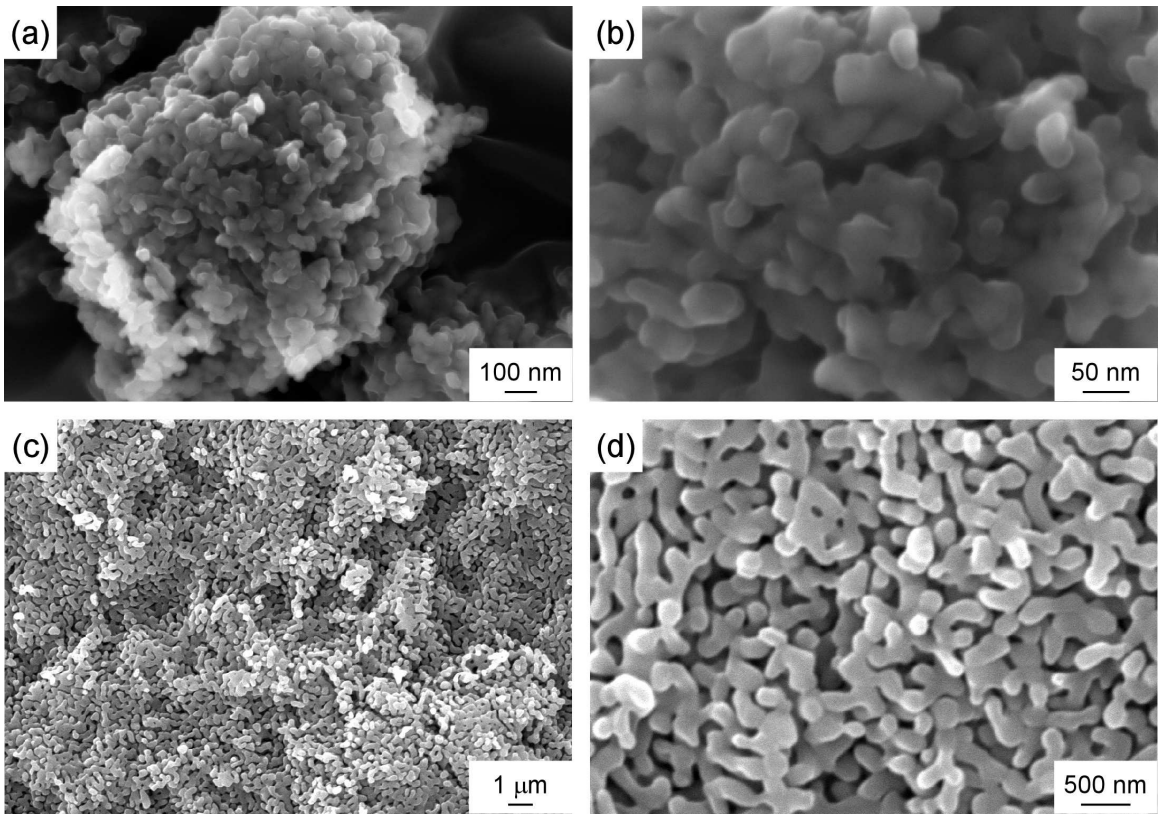

Figure 4. FE-SEM images of raw nano-Al_2O_3 powders (a), (b) and Al_2O_3 sintered body (c), (d)

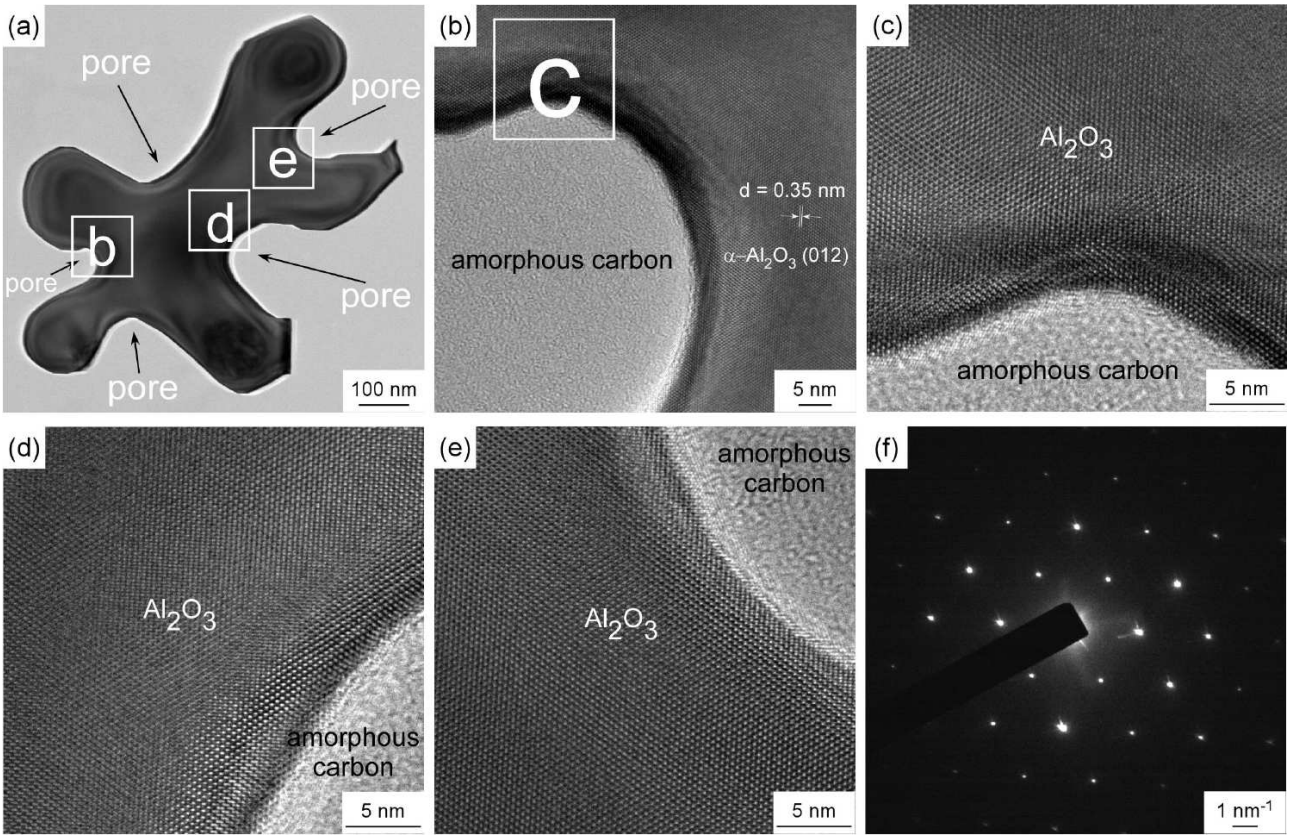

Figure 5. TEM image (a), HR-TEM images (b, c, d, e) and the selected area electron diffraction (SAED) (f) of microwave sintered Al_2O_3 body at 1673 K

posed to CO_2 and H_2O gases (Fig. 2), left large pores and no residuals of PLA template were observed after sintering.

Figure 5 shows the TEM micrographs and selected area electron diffraction of the Al_2O_3 sintered body. The porous structure of the Al_2O_3 sintered body with the average grain size of 100–150 nm was obtained (Fig. 5a). The high-resolution TEM (HR-TEM) pictures shown in Figs. 5b-e confirmed that the porous Al_2O_3 sintered body has single crystal structure. According to the PDF card #10-0173, the interplanar distance of 0.35 nm was attributed to α-Al_2O_3 plane (012). The interplanar distance data in Fig. 5 matched well with the XRD peak of $2\theta = 25.6°$ as shown in Fig. 3b. In microwave sintering, grain boundaries are common phenomenon in sintering neck region [13]. However, no grain boundaries in sintering neck of porous Al_2O_3 were found as shown in Fig. 5. It may be caused by suitable heating rate and enough space for mass transport by volume diffusion in Al_2O_3 microwave sintering.

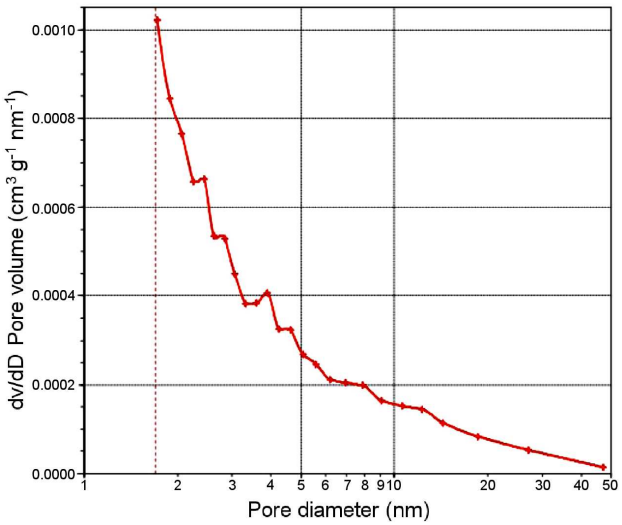

Figure 6. Pore diameter distribution of Al_2O_3 body microwave sintered at 1673 K determined by BJH method from low-temperature nitrogen desorption data

The mesoporous structure with pores between 1.7 and 50 nm was analysed from data measured by low-temperature nitrogen adsorption. The pore size distribution of the sintered Al_2O_3 body, determined according to the BJH method, of the mesoporous structure is shown in Fig. 6. The specific surface area, cumulative pore volume and average pore diameter of this mesoporous structure are 3.82 m^2/g, 0.0073 cm^3/g and 7.6 nm, respectively. Thus, according to the SEM analyses and low-temperature nitrogen adsorption testing, it is obvious that the Al_2O_3 body obtained by microwave sintering at 1673 K for 20 min, has not only macroporous structure (with pores of about 100 to 300 nm), but also mesoporous structure. The H_v of the Al_2O_3 sintered body was 1.254 ± 0.039 GPa.

IV. Conclusions

Macroporous and mesoporous Al_2O_3 sintered body was prepared using mesh screening shaped polylactic acid (PLA) template filled with nanosized Al_2O_3 powder and microwave sintered at 1673 K. During the sintering, the PLA template was decomposed and left large pores for promoting sintering of Al_2O_3. Macroporous structure of the Al_2O_3 sintered body consists of pores with diameter of 100–300 nm and the grain size of 100–150 nm. Local Al_2O_3 regions show single crystal structure and the average pore diameter of mesoporous structures in Al_2O_3 sintered body was about 7.6 nm. The Vickers hardness of the porous Al_2O_3 was 1.254 ± 0.039 GPa. The 3D-printed PLA template assisted microwave sintering is a promising processing technique for macroporous and mesoporous Al_2O_3 with local single crystal structure. This process has a promising application for porous materials with complex shape without material removal processes in the later steps. The porous Al_2O_3 prepared by this method has potential applications for complex shaped filters, catalyst supports, etc.

Acknowledgement: This research was supported by National Natural Science Foundation of China (No. 11747133), the Excellent Dissertation Cultivation Funds of Wuhan University of Technology (2018-YS-058) and the Doctoral Scientific Research Foundation of Wuhan University of Technology (No. 40120233). The authors would like to acknowledge Dr. Zhao Deng of Materials research and testing center of Wuhan University of Technology for the HR-TEM testing.

References

1. P. Sepulveda, J.G.P. Binner, "Processing of cellular ceramics by foaming and in situ polymerisation of organic monomers", *J. Eur. Ceram. Soc.*, **19** [12] (1999) 2059–2066.
2. E.C. Hammel, O.L.-R. Ighodaro, O.I. Okoli, "Processing and properties of advanced porous ceramics: An application based review", *Ceram. Int.*, **40** [10] (2014) 15351–15370.
3. S. Deville, E. Saiz, A.P. Tomsia, "Ice-templated porous alumina structures", *Acta Mater.*, **55** [6] (2007) 1965–1974.
4. R. Liu, T. Xu, C. Wang, "A review of fabrication strategies and applications of porous ceramics prepared by freeze-casting method", *Ceram. Int.*, **42** [2] (2016) 2907–2925.
5. J. Luyten, S. Mullens, I. Thijs, "Designing with pores – Synthesis and applications", *Kona Powder Part. J.*, **28** [131] (2010) 131–142.
6. Z. Fan, M. Lu, H. Huang, "Selective laser melting of alumina: A single track study", *Ceram. Int.*, **44** [8] (2018) 9484–9493.
7. Y. Gao, X. Xu, Z. Yan, G. Xin, "High hardness alumina coatings prepared by low power plasma spraying", *Surface Coatings Technol.*, **154** [2-3] (2002) 189–193.
8. F. Jay, V. Gauthier, S. Dubois, "Iron particles coated with alumina: Synthesis by a mechanofusion process and study of the high-temperature oxidation resistance", *J. Am.*

Ceram. Soc., **89** [11] (2006) 3522–3528.
9. J. Luyten, S. Mullens, J. Cooymans, A.M. Wilde, I. Thijs, R. Kemps, "Different methods to synthesize ceramic foams", *J. Eur. Ceram. Soc.*, **29** [5] (2009) 829–832.
10. Y. Tang, M. Mao, S. Qiu, K. Zhao, W. Chen, "Fabrication of porous alumina by directional freeze casting and annealing in TBA-water-sucrose system", *Ceram. Int.*, **44** [14] (2018) 17566–17570.
11. A.P. Li, F. Muller, A. Birner, K. Nielsch, U. Gosele, "Hexagonal pore arrays with a 50–420 nm interpore distance formed by self-organization in anodic alumina", *J. Appl. Phys.*, **84** [11] (1998) 6023–6026.
12. S.H. Huang, P. Liu, A. Mokasdar, L. Hou, "Additive manufacturing and its societal impact: A literature review", *Int. J. Adv. Manuf. Technol.*, **67** [5-8] (2013) 1191–1203.
13. K.I. Rybakov, E.A. Olevsky, E.V. Krikun, "Microwave sintering: Fundamentals and modeling", *J. Am. Ceram. Soc.*, **96** [4] (2013) 1003–1020.
14. R.E. Drumright, P.R. Gruber, D.E. Henton, "Polylactic acid technology", *Adv. Mater.*, **12** [23] (2000) 1841–1846.